Aust. Met. Mag. 54 (2005) 91-102

Long-term variations in winter rainfall of southwest Australia and the African monsoon

Peter G. Baines
Department of Civil and Environmental Engineering, University of Melbourne, Australia

(Manuscript received January 2004; revised November 2004)

The rainfall of southwest Western Australia (SWWA) suffered a 20 per cent long-term decrease in the late 1960s, which continues to the present day. This change approximately coincides with the well-known long-term decrease of rainfall in the African Sahel. It is shown here that these two substantial changes appear to be connected by conventional atmospheric dynamics, the former change being a consequence of the latter, as follows. The decrease in the Sahel rainfall and intensity of the African monsoon in the southern hemisphere winter (June, July, August) caused a corresponding decrease in the transport in the upper-level Hadley cell west of Africa. This in turn caused a decrease in the transport of the subtropical jet stream (STJS) which marks the southernmost extent of the Hadley circulation, and a southward movement of the main band of westerlies in the lower troposphere. These variations were continued eastward across the Indian Ocean, where they acted to reduce the rainfall over SWWA through reduced baroclinicity and the associated southward displacement of weather systems. Hence it appears that the long-term SWWA rainfall variations were directly related to the rainfall variations in the African monsoon, though variations of both these quantities on the interannual time-scale are affected by other factors. The change in Sahel and SWWA rainfall in the late 1960s may be seen as part of a coordinated rapid global change that will be discussed in detail elsewhere.

Introduction

The rainfall in southwest Western Australia (SWWA) mostly falls in May to September, and predominantly in June, July and August (JJA). Records show that, prior to the 1960s, this area had the most reliable rainfall in the country, but in the late 1960s a decrease of approximately 20 per cent (from approximately 3.8 mm/day to 3 mm/day for JJA) occurred in the long-term mean (IOCI 2002), which persists to this day and is largely unexplained (Fig. 1). So far, explanations for this long-term change have been sought from processes in the equatorial Pacific, from sea-surface temperatures in the Indian Ocean, and from greenhouse warming (IOCI 2002). This rainfall record may be compared with the rainfall in the African Sahel (Fig. 2). Here a decrease in excess of 0.4 mm/day

Corresponding author address: Peter G. Baines, Department of Civil and Environmental Engineering, University of Melbourne, Vic. 3010, Australia.
Email: pbaines@unimelb.edu.au

Fig. 1 **Annual values of the nett rainfall in the southwest corner of Australia over the winter period JJA, southwest of a direct line joining (30ºS, 115ºE) and (34ºS, 120ºE). This is based on an archive described by Jeffrey et al. (2001), based on the careful interpolation of daily data supplied by the Australian Bureau of Meteorology.**

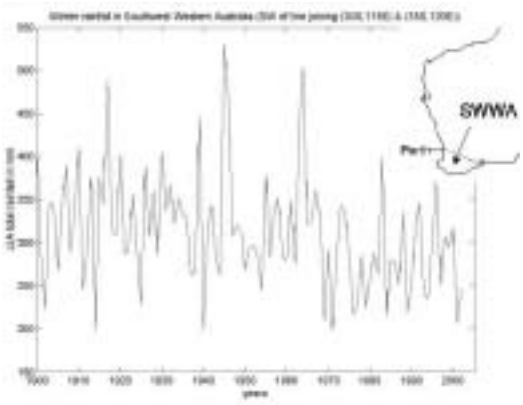

Fig. 2 **Rainfall for the season JJA for the African Sahel (here taken as the region 10º-20ºN, 10ºW-25ºE), shown dashed, obtained from the website of M. Hulme, Climate Research Unit, Univ. of East Anglia, and the SWWA rainfall of Fig. 1. These data have been normalised by their respective means and standard deviations. The correlation coefficient between them for the region where they overlap is 0.33.**

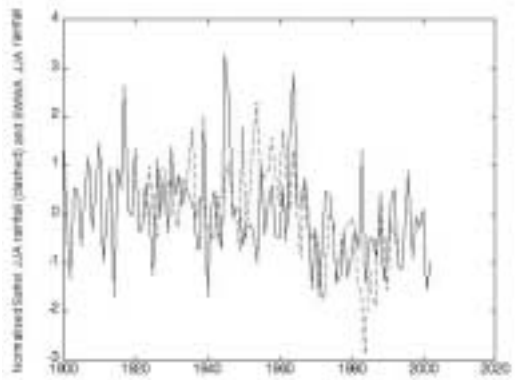

occurred for JJA in the region between 10° and 20°N, west of 34°E (Hulme 1992). The area of the rainfall change in the latter region is much larger than the former, and both records show a lot of interannual variability, but the salient point is that the rainfall records in both regions show a substantial and approximately coincident decrease in the late 1960s. It is argued here that these two changes are connected, and that the decrease in SWWA is a consequence of the changes that have caused the decrease in the African Sahel. The argument is a circumstantial and descriptive one, based on a chain of correlated connections between dynamically linked variables, but taken overall appears quite convincing.

The atmospheric data used for this study are primarily from the National Centers for Environmental Prediction (NCEP)/National Center for Atmospheric Research (NCAR) reanalysis dataset (Kalnay et al. 1996; Kistler et al. 2001), which is broadly consistent (Trenberth et al. 2000) with the corresponding independent reanalysis ERA15 from the European Centre for Medium-Range Weather Forecasts (ECMWF) for the time periods where these overlap. These have been supplemented with area-averaged rainfall data for Africa (Hulme (1994), with updates) and SWWA (Jeffrey et al. 2001). A brief description of the African monsoon, which is the principal driver of the African rainfall in the JJA season, is given below, followed by a description of the dynamical consequences of this monsoon and the connections with mid-latitude Australian rainfall. The first part of this discussion is reasonably straightforward meteorology, but it needs description here to provide the basis for the changes discussed later.

The African monsoon

As with other tropical regions, the rainfall in Africa varies substantially with the seasons. The region of maximum rainfall migrates in latitude with the seasons, so that it occurs in the summer hemisphere. It is largest during the northern hemisphere summer (June, July and August, denoted JJA), where it is associated with the African, or West African, monsoon, which occurs in the same season as the Indian monsoon. The meteorology of this region is complicated. It has been studied extensively over the past four decades, and this attention is continuing via, for example, the CLIVAR programme. During JJA, warm moist air from the equatorial Gulf of Guinea flows northward and eastward and feeds cumulus convection and precipitation in the intertropical convergence zone (ITCZ). The picture is complicated by the presence of the tropical easterly jet at the level of the tropopause, the African easterly jet, centred near 15°N, and the development of ‘easterly waves’ in this environment (see for example Grist and Nicholson (2001)). These waves organise and increase the precipitation and are

larger and more prominent in wetter seasons. They propagate westward over the Atlantic Ocean, where some of them may develop into tropical cyclones that impact on the American hemisphere (Gray 1990).

Figure 3 shows the global rainfall in the JJA season for the ten-year period 1958-1967, which we take as a reference period for conditions before the changes under discussion. It is clear that the North African rainfall constitutes a local maximum within a longitude band of approximately 90°, extending from 40ºW to 50ºE. This rainfall maximum is not as large as that associated with the Indian monsoon, which is centred on the Bay of Bengal and the Indian subcontinent, or that in the American hemisphere, centred on Central and northern South America and the Caribbean. However, as a region of convergence and precipitation it is dominant in the sector comprising Africa, the eastern Atlantic and the western Indian Ocean.

The Sahel region of North Africa occupies, approximately, the latitudinal band between 10° and 20°N latitude. This region is on the northern side of the maximum in seasonal (JJA) rainfall and is significantly affected by any variations in it. The annual rainfall in this region underwent a substantial decrease centred on the late 1960s, as shown in Fig. 2. The reasons for this have been much studied, and the decrease has been variously attributed to desertification (Charney et al. 1975; Xue and Shukla 1992), changes in sea-surface temperature (Folland et al. 1986; Rowell et al. 1992), or both (Giannini et al. 2003). Our concern here, however, is not so much the causes of this change, but the consequences of it, since rainfall is a measure of the local heating of the atmosphere via latent heat release. Figure 2 shows the rainfall as inferred from a network of ground stations (Hulme 1994). This is preferred to the rainfall as inferred from the NCEP reanalysis, since the latter is a derived variable in this dataset, and regarded as less reliable than others such as pressure and winds (Kalnay et al. 1996).

The Hadley circulation and subtropical jet stream

In JJA, the zonal mean meridional circulation that is normally termed the ‘Hadley circulation’ rises north of the equator and descends south of the equator, with the reverse in December to February (Peixoto and Oort 1992). Examination of the longitudinal structure of this circulation shows that the rising motion and upper-level divergence is concentrated in the principal regions of latent heat release (Waliser et al. 1999; Trenberth et al. 2000), shown in Fig. 3. Figure 4(a)

Fig. 3 The spatial pattern of mean rainfall for the reference period 1958-1967 for the JJA season (from NCEP reanalysis).

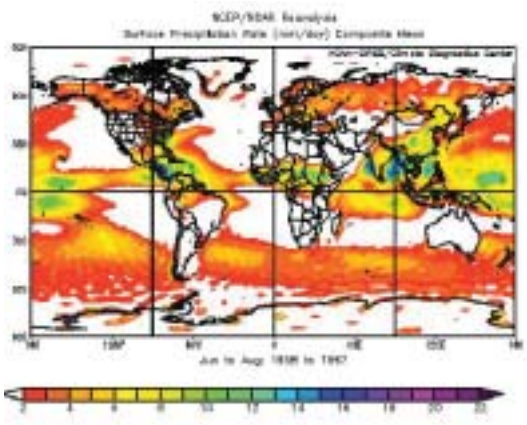

shows the meridional motion at the upper level (200 hPa) for JJA for 1958-67. Southward motion can be clearly seen at the 200 hPa level, south of the main regions of tropical rainfall, and these constitute the upper part of the Hadley circulation, which appears distinctly longitudinally ‘lumpy’. The largest maximum is over the Indian Ocean, forced by the Indian monsoon, which is contiguous with the region of southward motion east of Australia over the west Pacific. A second major region of southward motion occurs over (and to the west of) South America, and the third is south of the African monsoon rainfall region. All of these regions of southward flow terminate at approximately 30°S. The return northward flow (not shown here) at low levels is much more spread out, with the exception of the concentrated East African Jet (described, for example, by Gill (1982)) to the east of the Ethiopian mountains, which feeds the Indian monsoon.

Figure 4(b) shows a vertical section of north-south velocity across 20°S, from 60°W to 120°E longitude, of the flow shown in Fig. 4(a). The strong southward-moving airstream centred on 200 hPa on the Greenwich meridian is the Hadley circulation emanating from the African monsoon region. The broader region between 30°E and 110°E similarly emanates from the Indian monsoon – west Pacific convection region. Note that this southward-moving air is at high levels, having been heated by latent heat release. The northward return flow has generally lower velocity and occupies a much broader range of heights throughout the troposphere.

Fig. 4 **(a) The spatial pattern of the meridional (north-south) wind field at 200 hPa for the reference period 1958-1967 for the JJA season. Note the four principal regions of the southern Hadley circulation. (b) A longitude height section at 20°S, from 60°W to 120°E, showing the north-south velocity. The dark region centred at 200 hPa on the Greenwich meridian denotes the southward motion in the upper branch of the Hadley circulation from the African monsoon region. Both figures from NCEP reanalysis.**

(a)

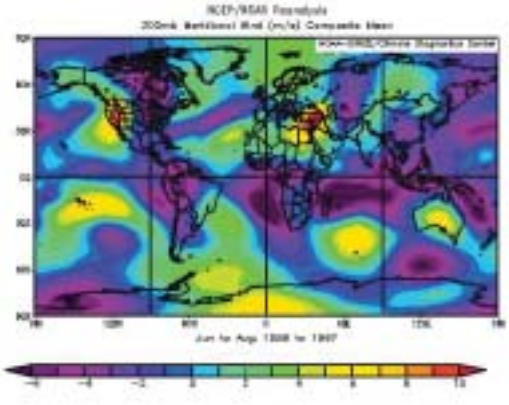

(b)

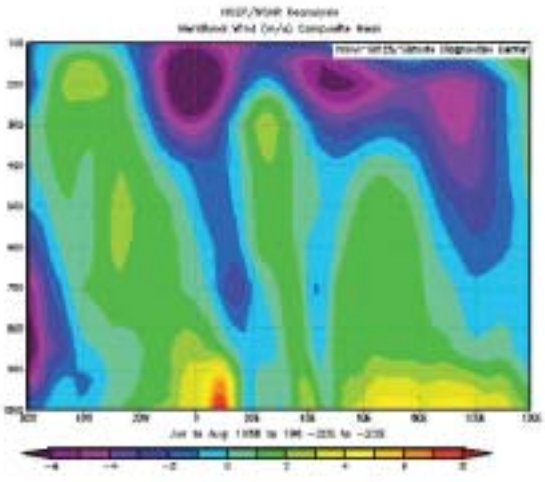

The upper levels of the Hadley circulation carry air with high potential temperature southward. However, as is well known, this circulation becomes dynamically unstable south of 30°S through the process of baroclinic instability (Holton 1979; Gill 1982). As this upper-level air moves southward, being well-separated from the ground it approximately conserves its mean angular momentum; its perpendicular distance from the earth's axis of rotation progressively decreases, and it acquires an increasingly large velocity toward the east. This is manifested in the subtropical jet stream, which is a very prominent feature of the zonal wind field for JJA at 200 hPa shown in Fig. 5(a), centred near 30°S. This sets up the large vertical shear in the zonal wind which is dynamically unstable, producing eddies of the synoptic scale which dominate the motion further south throughout the troposphere. These eddies transport the heat that is carried southward by the Hadley circulation at lower latitudes, with the change-over occurring near 30°S. One can see that the increases in the strength of the jet stream with longitude (in Fig. 5(a)) roughly correspond with the regions of southward motion shown in Fig. 4(a), which seems remarkable on this 10-year time average. Examination of instantaneous versions of these figures shows much more variation: large eddies centred to the south of 30°S are prominent, and advect the subtropical jet stream around their northern extremities. Averages of time-scales of a month or more, however, give pictures that resemble Figs 4 and 5.

Figure 5(b) shows the low-level zonal flow at 850 hPa for JJA for 1958-67. The broad maximum in eastward velocity between 30°W and 120°E centred near 45°S is identified with the main southern hemisphere winter storm track. Consistent with geostrophy, this is the range of longitudes where the north-south temperature gradient is (relatively) large, and this is because the southward heat flux, fed by equatorial processes and the Hadley circulation to the north, is also large. There are many other details that may be identified in Figs 3 to 5, but the above are sufficient for the purposes of the present discussion. The principal point is that the salient properties of the atmospheric flow in mid-latitudes in this sector are dependent on the processes in the equatorial regions to the north, particularly the rainfall. The interested reader may gain more familiarity with all of these quantities by downloading any number of related colour pictures from the NCEP website (starting from http://www.cdc.noaa.gov/cgibin/Composites/printpage.pl).

Changes in the atmospheric circulation across the late 1960s

The foregoing discussion gives a brief description of the mean atmospheric flow for JJA for 1958-1967. The differences in the same variables that are noticed if one takes an average over the 30-year period 1971-2000 are described next. The length of this period is

Fig. 5 **(a) Zonal flow at 200 hPa for JJA for 1958-1967, to complement the meridional flow of Fig. 4(a). Note the subtropical jet stream centred on 30ºS. (b) The same but at 850 hPa. Note the strong storm track across the Indian Ocean sector. Both figures are from NCEP reanalysis.**

(a)

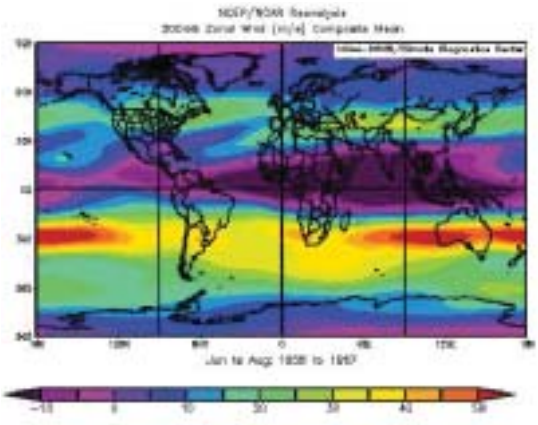

(b)

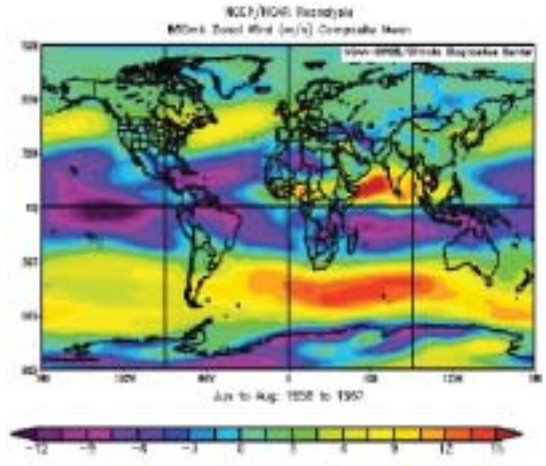

Fig. 6 **The spatial pattern of the difference in rainfall for JJA for the 30-year period 1971-2000, relative to that of 1958-1967, shown in Fig. 3. Data from NCEP reanalysis.**

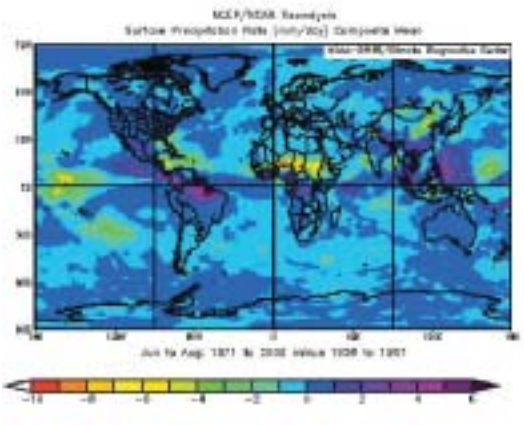

not important, and the same differences are perceived if, for example, the period 1971-1980 is taken instead. The longer period is preferred here as it helps to make the point that the changes are long-standing. The spatial structure is considered first, followed by the temporal variation of key variables. Figure 6 shows the difference in the rainfall. There are regions of increase in the Amazon basin and the west Pacific, and regions of decrease in the central Pacific and the African Sahel region. The latter region is the one of interest here, and it reflects the changes seen in Fig. 2.

Figure 7(a) shows the difference between the north-south velocity in the upper-level Hadley circulation at 200 hPa. The most striking feature is the large decrease in the African branch, accompanying the decrease in latent heat release over the Sahel that appears to have caused it. The decrease also appears in the section at 20°S, shown in Fig. 7(b). Corresponding changes in the zonal flow are shown in Fig. 8. There is a decrease in the strength of the subtropical jet stream (STJS) over the Indian Ocean sector (Fig. 8(a)), consistent with the large decrease in the African Hadley circulation, following the connection described in the previous section. Note that, in this figure, this decease is initially large in the African sector and is then maintained over most of the Indian Ocean sector as changes in the Hadley circulation forced by the Indian Monsoon, averaged over this period, are seen to be small. The difference in STJS transport decreases over Western Australia, where the anomaly in the Hadley circulation shown in Fig. 7(a) has increased southward flow. The difference in the low-level zonal flow (850 hPa) shown in Fig. 8(b) shows that the eastward flow has generally decreased north of 45°S and increased south of this latitude, implying that the main storm track has moved south, relative to the period 1958-67. This applies across the whole of the Indian Ocean sector, but is stronger in the east. A southward-displaced storm track is consistent with reduced rainfall in SWWA.

Fig. 7 **As in Fig. 4, but showing the difference between the periods 1971-2000 and 1958-1967. (a) Meridional flow at 200 hPa. (b) Meridional flow across a longitude-height section at 20ºS, from 60ºW to 120ºE. Data from NCEP reanalysis.**

(a)

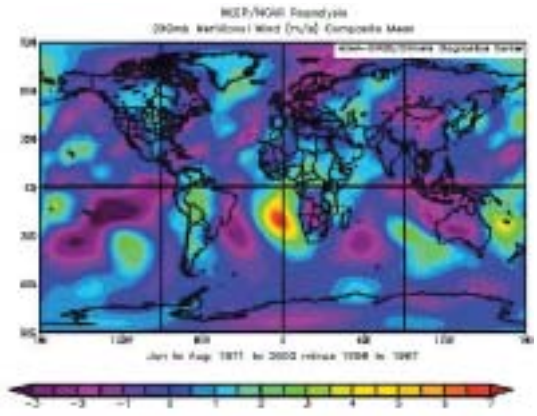

(b)

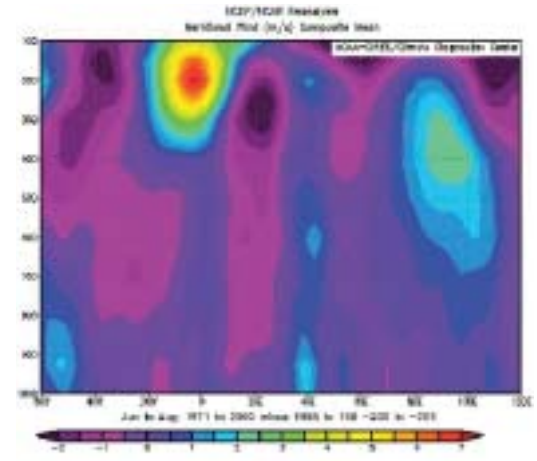

Fig. 8 **As in Fig. 5, but showing the difference between the periods 1971-2000 and 1958-1967. (a) Zonal flow at 200 hPa. (b) Zonal flow at 850 hPa. Data from NCEP reanalysis.**

(a)

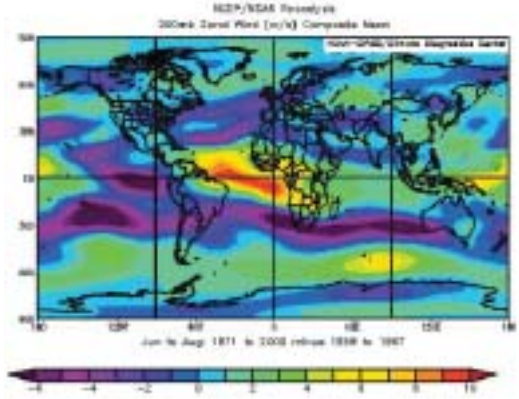

(b)

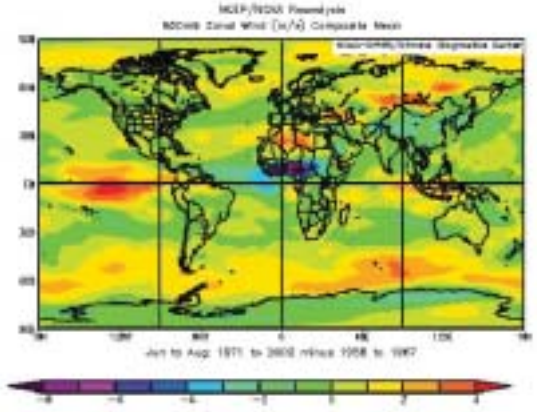

Figures 6 to 8 give some idea of the spatial structure of the changes that have occurred. We now examine the temporal behaviour of the changes that relate to SWWA by analysing time series of several of the key variables involved. These time series have been decomposed using the empirical mode decomposition method of Huang et al. (1998, 1999), which involves fitting envelopes to each of the maxima and the minima of the data and subtracting the mean of these envelopes to give a residual. This procedure may be repeated several times, but here is only carried out once to isolate and remove the first intrinsic mode function (IMF), which is the high frequency part of each signal (here denoted c_1 for each record). Here a quadratic fit q has been fitted to and subtracted from the data before the decomposition is done, after which it is added to the residual, r_1. In each case the initial data are equal to this c_1 component, plus the low-frequency residual that is the main interest. These data are displayed in Fig. 9. The first column shows the raw record with one value for each year. The second column contains the c_1 component, which has zero local mean, and contains the high frequency (interannual) part of each signal. The final column shows values of $q + r_1$, which is the difference between the raw data and c_1, i.e. column 1 minus column 2, and describes the low frequency, or interdecadal variability.

Fig. 9 **Time series of key variables. All of these have been decomposed using the empirical mode decomposition procedure as described in the text, and normalised with their standard deviation. The first column is the basic JJA record for each year, the second is the interannual variation with zero local mean, and the third is the residual low frequency variation. (a) JJA rainfall in the African Sahel, as in Fig. 2; (b) mass transport in the upper branch of the Hadley circulation, integrated over the range 20ºW to 15ºE, 500 to 100 hPa; (c) mass transport in the subtropical jet stream at 10ºE, integrated over the range 20ºS to 40ºS, 500 to 100 hPa; (d) as for (c) but at longitude 90ºE; (e) JJA rainfall in SWWA, as in Fig. 1. The vertical dashed line in the figures in the last panel denotes the year 1970.**

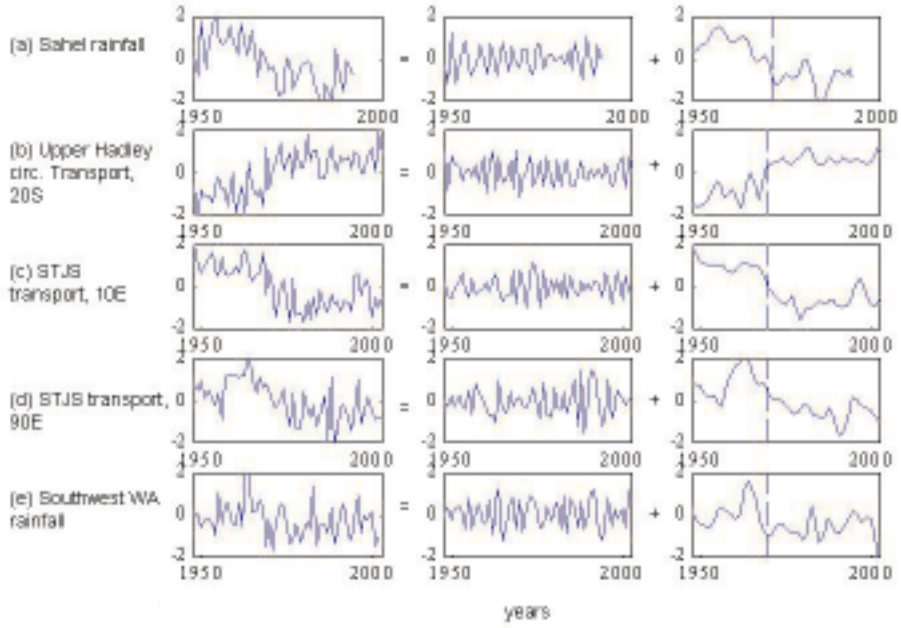

Figure 9 shows a sequence of five time series decomposed in this manner, all for the JJA season. The first is the Sahel rainfall record, the second the transport in the upper African branch of the Hadley circulation, the third and fourth the transport in the STJS at 10ºE and at 90ºE, and finally, the rainfall record for southwest Australia. All of these records show a substantial change in the late 1960s, which is made more visible after the removal of the high frequency (interannual) component. These low frequency records have maximum correlation at or near zero lag, and the values are given in Table 1. Consistent with conventional meteorology, the chain of causality runs as follows. Changes in the rainfall in the Sahel associated with the African monsoon imply corresponding changes in the latent heating of the atmosphere in this region. This causes changes in the upper-level African branch of the Hadley circulation, which in turn causes the changes in the STJS to the south. This affects the strength of the STJS to the east, across the Indian Ocean, as reflected by the record at 90ºE. The latter is also affected by any changes in the Indian monsoon, but as Fig. 6 indicates, these are relatively small on the decadal time-scales over the period under discussion.

The final record in Fig. 9 is the SWWA rainfall, which shows the same low frequency variation as the other records. Here the mechanics of the chain of causality are less obvious, but may be stated in general terms. Most of the rainfall in SWWA in JJA is associated with cold frontal systems that impact from the southwest, and are components of the synoptic environment over the Southern Ocean (IOCI 1999, 2001, 2002). As implied by Fig. 5, the mean westerly wind over the Indian Ocean sector at this time of year consists of the upper-level STJS centred near 30ºS at 200 hPa, and the broad low-level westerly wind stream centred near 45ºS. As is suggested by changes in Fig. 8(b), the NCEP reanalysis data imply that this westerly wind stream moved south during the late 1960s. To represent this, a time series of the zonal wind at 90ºE at 850 hPa has been taken across the range of latitudes 30ºS to 60ºS. A time series of the latitude of the centroid of this wind profile has been computed according to:

Table 1. Correlation coefficients between the low frequency residual records ($q + r_1$), shown in Figs 9 and 10, at zero lag. A negative correlation between the latitude of the centroid of the zonal wind at 90ºE and (for example) rainfall implies that the centroid moves south as rainfall increases.

$q + r_1$		*Sahel rain*	*Southward transport upper Hadley cell 20ºS*	*Eastward transport STJS 10ºE*	*Eastward transport STJS 90ºE*	*Latitude of centroid of zonal wind 850 hPa 90ºE*	*SWWA rain*
		JJA	*JJA*	*JJA*	*JJA*	*JJA*	*JJA*
Sahel rain	JJA	1	0.75	0.78	0.60	-0.45	0.38
Southward transport upper Hadley cell 20ºS	JJA	0.75	1	0.89	0.69	-0.55	0.4
Eastward transport STJS 10ºE	JJA	0.78	0.89	1	0.76	-0.62	0.54
Eastward transport STJS 90ºE	JJA	0.60	0.69	0.76	1	-0.81	0.63
Latitude of centroid of zonal wind 850 hPa 90ºE	JJA	-0.45	-0.55	-0.62	-0.81	1	-0.69
SWWA rain	JJA	0.38	0.40	0.54	0.63	-0.69	1

$$\bar{y}(t)\int_{60°S}^{30°S} u(y,t)dy = \int_{60°S}^{30°S} yudy \qquad ...1$$

where y denotes latitude. This time series is shown in Fig. 10, together with the low frequency component ($q+r_1$) shown dashed, and the latter is included in Table 1. There is a clear movement of about one half degree of latitude, or approximately 50 km, to the south of the westerly wind stream at 850 hPa over the late 1960s. This is not a large distance, but its significance lies in that it represents a southward change of the whole westerly wind stream, which is the main storm-track region in the southern hemisphere. Prior to 1970, the centroid was mostly north of 45ºS latitude, but afterward was mostly south of this, with a modest recovery during the 1990s, mirroring the rainfall curve of Fig. 1. In the environment upstream of SWWA, therefore, in the late 1960s the STJS that passes overhead weakened, and the main westerly wind stream moved south. The latter, in particular, may be expected to cause the rain-bearing systems to also be displaced southwards, including those that impact on SWWA, and this variable has the largest correlation with low frequency SWWA rainfall of all the variables in Table 1.

The southward displacement of the mean westerlies is consistent with well-known atmospheric dynamics. The formation of synoptic-scale disturbances in the storm track region occurs through baroclinic instability of the background flow. The decrease in African rainfall and mass transport in the African Hadley circulation implies that, in this longitude sector, there is a corresponding decrease in the southward flux of heat from the tropics into and across the mid-latitudes. Consistent with this, the reanalysis data show there is a decrease in the mean mid-latitude north-south temperature gradient (not shown here). The thermal wind equation then implies a decrease in the vertical wind shear, which is certainly evident in the vicinity of the STJS. From the two-layer theory of baroclinic instability (Phillips 1954; Holton 1979; Baines and Frederiksen 1978), the flow is unstable if the eastward zonal wind difference between the upper and lower layers exceeds

Fig. 10 Time series of the latitude of the centroid of the mean westerly wind stream at 90ºE, 850 hPa between 30ºS and 60ºS from 1948 to 2003 for JJA, from NCEP reanalysis. The dashed line denotes the low frequency behaviour (q+r_1) as in Fig. 9.

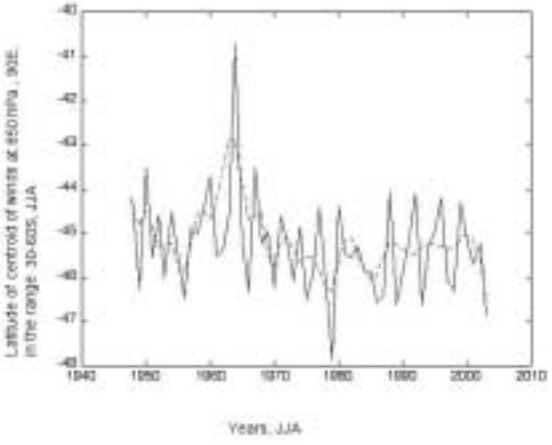

$$\frac{0.124 C_p \Delta\theta}{2a\Omega} \frac{\cos\phi}{\sin^2\phi} \qquad ...2$$

where ϕ denotes latitude, a and Ω denote the Earth's radius and angular velocity, C_p the specific heat of air at constant pressure, and $\Delta\theta$ the vertical difference in potential temperature between the upper and lower layers. Baroclinic instability occurs because of the interaction of a baroclinic wave in the upper troposphere with a corresponding baroclinic wave in the lower troposphere, and Eqn 2 is essentially a condition for these two waves to be relatively stationary for a suitable wavelength. The β-effect works to prevent this, and it is manifested through the dependence on latitude, which becomes stronger at lower latitudes. Since $\Delta\theta$ varies very little, a decrease in the vertical shear implies that the instability and consequent eddies occur at higher latitude, namely further south.

Interannual variability

In the above analysis, the interannual c_1 components have been removed from the discussion. One may ask how well the chain of causality identified for the low frequency components applies to them, and we consider this here. The correlation coefficients for c_1 are shown in Table 2. These numbers are again all at zero lag, and the correlations decrease to values that are small or of opposite sign if they are repeated with lags of just one or two years, as would be expected. These figures present a slightly different story from those in Table 1. In particular, the connection between the Sahel rainfall and the Hadley cell transport has completely disappeared. However, Sahel rainfall is still correlated with the STJS transport and the latitude of the tropospheric winds at 90ºE. Both of these are still correlated with the SWWA winter rainfall, implying that the interannual variability in the latter is still dependent on the dynamics of the westerly airstream to the west. Correlation plots of the zonal wind at 200 and 850 hPa with component c_1 for the Sahel JJA rainfall (Figs 11(a) and (b) respectively) show significant regions of correlation in the southeast Indian Ocean, so that even at interannual time-scales these variables are still related to the Sahel rainfall. All variables in Table 2 have some degree of correlation with the Southern Oscillation Index, and this includes both the SWWA and the Sahel rainfall. This implies that dynamical processes associated with ENSO (El Niño-Southern Oscillation) affect both of these regions on the interannual time-scale, as is well known (see for example Rowell (2001)), but this influence is not manifested via the African branch of the Hadley circulation.

Conclusions and discussion

A descriptive analysis of factors that affect the long-term rainfall of SWWA has been carried out and has shown that the major decrease that occurred in the late 1960s in JJA can be traced back to a decrease in the intensity of the African monsoon. This link is consistent with well-known principles of atmospheric dynamics – the Hadley circulation, conservation of angular momentum, the subtropical jet stream, and the stability of the zonal wind field across the Indian Ocean. The decrease that occurs in SWWA rainfall is manifest in all the variables in the chain of connections extending back to the Sahel, with correlation decreasing with distance along the chain. However, this link is not apparent on the interannual time-scale, as the rainfall in both regions may be affected by other factors such as ENSO. The principal breakdown in the correlation chain on the interannual time-scale is in the Hadley circulation transport. On these time-scales, this transport shows significant correlation with South American (Brazilian) rainfall (not shown here but see Fig. 6). This helps to emphasise that these changes during the 1960s are not restricted to the African and Indian Ocean sector, and are part of a global pattern of change that will be described more fully elsewhere (Baines and Folland, unpublished work), and of which the Sahel rainfall is only a component.

Table 2. Correlation coefficients between the 'high frequency' records (c_1) for the variables in Table 1 at zero lag, plus the Southern Oscillation Index (SOI), for the season JJA. A negative correlation between the latitude of the centroid of the zonal wind at 90ºE and (for example) rainfall implies that the centroid moves south as rainfall increases.

c_1		*Sahel rain*	*Southward transport upper Hadley cell 20ºS*	*Eastward transport STJS 10ºE*	*Eastward transport STJS 90ºE*	*Latitude of centroid of zonal wind 850 hPa 90ºE*	*SWWA rain*	*SOI*
		JJA	*JJA*	*JJA*	*JJA*	*JJA*	*JJA*	*JJA*
Sahel rain	JJA	1	-0.11	0.205	0.38	-0.4	0.18	0.31
Southward transport upper Hadley cell 20ºS	JJA	-0.11	1	-0.26	0.10	-0.24	0.002	0.21
Eastward transport STJS 10ºE	JJA	0.205	-0.26	1	0.22	-0.08	0.30	0.31
Eastward transport STJS 90ºE	JJA	0.38	0.10	0.22	1	-0.65	0.59	0.24
Latitude of centroid of zonal wind 850 hPa 90ºE	JJA	-0.4	-0.24	-0.08	-0.65	1	-0.31	-0.21
SWWA rain	JJA	0.18	0.002	0.30	0.59	-0.31	1	0.39
SOI	JJA	0.31	0.21	0.31	0.24	-0.21	0.39	1

This work is dependent on the NCEP/NCAR reanalysis data for the atmospheric winds and transports, and on rain-gauge data for the rainfall. NCEP/NCAR data are known to be less reliable in the early years (particularly prior to 1958) and at high southern latitudes due to the sparsity of observations, and use of the data in these periods and regions has been avoided here as much as possible (Kalnay et al. 1996; Kistler et al. 2001). However, the data were employed in determining the mean latitude of the westerly wind stream in the main storm track centred on 45ºS. The results are, however, consistent with dynamics (via the NCEP model) and with all of the other variables that are mostly located north of 35ºS.

Other attempts to account for the SWWA rainfall decrease have been summarised in the IOCI-coordinated studies (IOCI 1999, 2001, 2002), and have involved:

(a) teleconnections from the equatorial Pacific, including the Southern Oscillation;
(b) the direct effects of modal patterns of sea-surface temperature, notably in the Indian Ocean; and
(c) greenhouse warming.

While all of these may have some influence, none of the associated studies has provided a strong case for their being the principal cause of the change in the 1960s. These will be discussed briefly in turn.

Teleconnections from the equatorial Pacific essentially consist of the El Niño-Southern Oscillation (ENSO) and its low-frequency component, the Pacific Decadal Oscillation (PDO). ENSO may be represented by the Southern Oscillation Index (SOI); this has an effect on the rainfall in both SWWA and the Sahel, but cannot account for the low frequency change as discussed in the previous section. The PDO, as represented by the PDO Index (e.g. Mantua and Hare 2002), underwent a change in sign in 1975. As shown above, the chain of changes centred on the late 1960s was effectively complete by 1970 (see Fig. 9). Moreover, the PDO shows more complex variability than the low frequency rainfall curves, so that correlations between the PDO and the rainfall of SWWA are low (typically < 0.2), regardless of the period taken or whether the original variable or the residual breakdown ($q+r_1$) is used. Correlations between the PDO and the other variables in the chain of connec-

Fig. 11 (a) A plot of the correlation coefficient of the zonal wind for JJA at 200 hPa (from NCEP data) with the time series for the interannual component (c1) of Sahel JJA rainfall shown in the top central panel of Fig. 9. (b) As for (a), but for the zonal wind at 850 hPa.

(a)

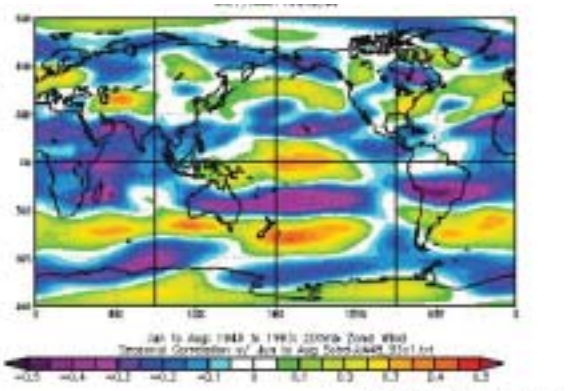

(b)

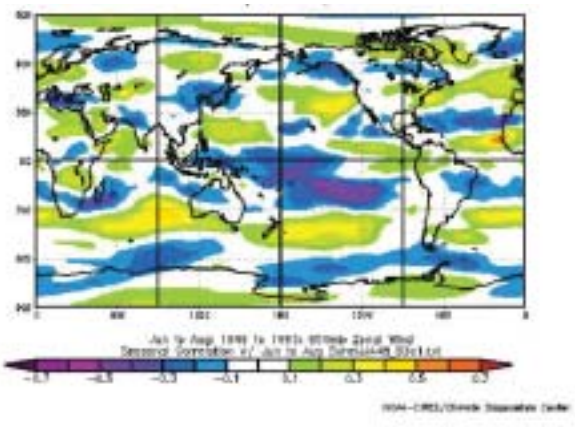

tions are, for the most part, even smaller than those with the rainfall variables. These reasons combined would seem to imply that the main SWWA rainfall decrease is not related to the PDO.

Correlations between patterns of Indian Ocean sea-surface temperature (SST) and SWWA rainfall have not revealed significant direct connections. Recent modelling studies of the effects of SST (Giannini et al. 2003; Bader and Latif 2003), particularly Indian Ocean SST, have, however, shown a significant effect on Sahel rainfall. The mechanism in the model is stated as follows. Cold anomalies in the tropical Indian Ocean prior to 1970 cause upper-level convergence in the overlying troposphere, which communicates via the equatorial wave guide to the African Sahel where it causes upper-level divergence, and hence more rainfall there. This implies that changes in Indian Ocean SSTs may be part of the cause of the 1960s rainfall changes in SWWA, but that the process works through the chain of connections described in this paper.

Recent model studies have shown that greenhouse warming may cause the main Indian Ocean storm track to move southward (e.g. IOCI 2002), but this does not explain why the main changes occurred in the 1960s rather than more recently. As far as explaining the main change in SWWA rainfall, therefore, the chain of processes described here would seem to be a strong competitor.

If variations in the strength of the winter (JJA) African monsoon have caused the decrease in rainfall in SWWA, what inferences can be made about the future long-term prospects for rain in this region? Is it possible that the intensity of the African monsoon in JJA could be reversed, thereby reversing the decrease of the 1960s? The cause of the rainfall decrease in the African Sahel has been debated for several decades, and appears to be associated with interhemispheric changes in sea-surface temperature, reinforced by consequent changes in land-surface properties (Giannini et al. 2003). In fact, it can be shown that these changes are part of a global pattern of changes in sea-surface temperature, tropical rainfall and associated circulation patterns that was centred on the late 1960s. There is as yet no clear sign that the pre-1960s environment will return in the near future.

Acknowledgments

The author would like to acknowledge discussions with colleagues at CSIRO Atmospheric Research where most of this work was performed, and in particular to Ian Smith, Graeme Pearman and Leon Rotstayn. He is also grateful for the constructive comments of Neville Nicholls and another anonymous referee, which led to significant improvements.

References

Baines, P.G. and Frederiksen, J.S. 1978. Baroclinic instability on a sphere in two-layer models. *Q. Jl R. Met. Soc., 104,* 45-68.

Bader, J. and Latif, M. 2003. The impact of decadal-scale Indian Ocean sea surface temperature anomalies on Sahelian rainfall and the North Atlantic Oscillation. *Geophys. Res. Let., 30,* CLM 7-1:4.

Charney, J., Stone, P. and Quirk,W. 1975. Drought in the Sahara: a biogeophysical feedback mechanism. *Science, 237,* 434-5.

Folland, C.K., Palmer, T.N. and Parker, D.E. 1986. Sahel rainfall and worldwide sea temperatures, 1901-1985. *Nature, 320,* 602-4.

Gill, A.E. 1982. *Atmosphere-Ocean Dynamics*. Academic Press, New York, 662 pp.

Gray, W.M. 1990. Strong association between West African rainfall and U.S. landfall of intense hurricanes. *Science, 249,* 1251-6.

Grist, J.P. and Nicholson, S.E. 2001. A study of the dynamic factors influencing the rainfall variability in the West African Sahel. *Jnl climate, 14*, 1337-59.

Giannini, A., Saravanan, R. and Chang, P. 2003. Ocean forcing of the Sahel rainfall on interannual and interdecadal time scales. *Science, 302*, 1027-30.

Holton, J. 1979. *An Introduction to Dynamic Meteorology*, Academic Press, 391 pp.

Huang, N.E., Shen, Z., Long, S.R., Wu, M.C., Shih, H.H., Zheng, Q., Yen, N., Tung, C.C. and Liu, H.H. 1998. The empirical mode decomposition and the Hilbert spectrum for nonlinear and non-stationary time series analysis. *Proc. Roy. Soc. A, 454*, 903-95.

Huang, N.E., Shen, Z. and Long, S.S. 1999. A new view of nonlinear water waves: the Hilbert Spectrum. *Ann. Rev. Fluid Mech., 31*, 417-57.

Hulme, M. 1992. Rainfall changes in Africa: 1931:1960 to 1961:1990. *Int. J. Climatol., 12*, 685-99.

Hulme, M. 1994. Century-scale time series of regional anomalies in Africa. In *Trends '93: A Compendium of Data on Global Change*, T.A. Boden, D.P. Kaiser, R.J. Stepanske, and F.W. Stoss (eds.), 964-73. ORNL/CDIAC-65. Carbon Dioxide Inf. Anal. Center, Oak Ridge Nat. Lab., Tenn, USA.

IOCI 1999. Towards understanding climate variability in south western Australia – *Research reports on the First Phase of the Indian Ocean Climate Initiative*, Indian Ocean Climate Initiative Panel, Perth, October 1999, 237 pp.

IOCI 2001. Second Research Report – Towards understanding climate variability in south western Australia. *Research reports on the Second Research Phase of the Indian Ocean Climate Initiative*. Indian Ocean Climate Initiative Panel, Perth, October 2001, 193 pp.

IOCI 2002. *Climate variability and change in south west Western Australia*, Indian Ocean Climate Initiative Panel, W.A. Dept. of Envir., Perth, Sept., 34 pp.

Jeffrey, S.J., Carter, J.O., Moodie, K.B. and Beswick, A.R. 2001. Using spatial interpolation to construct a comprehensive archive of Australian climate data. *Environmental Modelling and Software, 16*, 309-30.

Kalnay, E., Kanamitsu, M., Kistler, R., Collins, W., Deaven, D., Gandin, L., Iredell, M., Saha, S., White, G., Woollen, J., Zhu, Y., Leetmaa, A., Reynolds, B., Chelliah, M., Ebisuzaki, W., Higgins, W., Janowiak, J., Mo, K.C., Ropelewski, C., Wang, J., Jenne, R. and Joseph, D. 1996. The NCEP/NCAR 40-Year Reanalysis Project. *Bull. Am. Met. Soc., 77*, 437-71.

Kistler, R., Kalnay, E., Collins, W., Saha, S., White, G., Woollen, J., Chelliah, M., Ebisuzaki, W., Kanamitsu, M., Kousky, V., van den Dool, H., Jenne, R. and Fiorino, M. 2001. The NCEP-NCAR 50-year Reanalysis: monthly means CD-ROM and documentation. *Bull. Am. Met. Soc., 82*, 247-67.

Mantua, N.J. and Hare, S.R. 2002. The Pacific Decadal Oscillation. *J. Oceanography, 58*, 35-44.

Peixoto, J.P. and Oort, A.H. 1992. *Physics of Climate*, American Institute of Physics, New York, 520 pp.

Phillips, N.A. 1954. Energy transformations and meridional circulations associated with simple baroclinic waves in a two-level, quasi-geostrophic model. *Tellus, 6*, 273-86.

Rowell, D.P. 2001. Teleconnections between the tropical Pacific and the Sahel. *Q. Jl R. Met. Soc., 127*, 1683-706.

Trenberth, K.E., Stepaniak, D.P. and Caron, J.M. 2000. The global monsoon as seen through the divergent atmospheric circulation. *Jnl climate, 13*, 3969-93.

Waliser, D.E., Shi, Z., Lanzante, J.R. and Oort, A.H. 1999. The Hadley circulation: assessing NCEP/NCAR reanalysis and sparse in-situ estimates. *Climate Dynamics, 15*, 719-35.

Xue, Y. and Shukla, J. 1992. The influence of land surface properties on Sahel climate. Part I: desertification. *Jnl climate, 6*, 2232-45.